Estimate the Temperature Rise of Medium Voltage Metal Enclosed Switchgear by Simplified Heat Transfer Calculations

Fjeld, Elin[1]; Rondeel, Wilhelm G. J.[1]; Attar, Elham[2]; Singh, Shailendra[2]

[1]Department of Electrical engineering, Information Technology and Cybernetics - University of South-Eastern

[2]ABB AS

Fjeld, E., Rondeel, W. G. J., Attar, E., & Singh, S. (2020). Estimate the Temperature Rise of Medium Voltage Metal Enclosed Switchgear by Simplified Heat Transfer Calculations. *IEEE Transactions on Power Delivery, 36*(2), 853-860. https://doi.org/10.1109/TPWRD.2020.2995468

This is the accepted version of an article appearing in *IEEE Transactions on Power Delivery* and may appear differently than the finally published version.

Publisher's version: DOI: 10.1109/TPWRD.2020.2995468

Estimate the Temperature Rise of Medium Voltage Metal Enclosed Switchgear by Simplified Heat Transfer Calculations

Elin Fjeld, *Member, IEEE*, Wilhelm G. J. Rondeel, Elham Attar, and Shailendra Singh

***Abstract*-- Electrical equipment will experience a rise in temperature during normal operation. During a development process, prototypes and laboratory tests will be required to make sure the temperature rises are within acceptable limits as defined by standards. The aim of having a tool to predict the temperature rise, is to reduce the number of prototypes and test loops needed in the laboratory during a development period. Advanced simulation tools such as CFD can give valuable results, however, they require expertise user and extensive compute and manpower allocation. This paper presents a practical design approach developed for providing a first, quick and rough estimate of the temperature rise of the most critical parts in an air insulated switchgear. The main idea behind the method is to first use the method described in IEC 60890 to estimate the temperature rise of the gas inside the switchgear. Then, simplified heat transfer calculations are used to estimate the over-temperature of critical parts relative to the surrounding gas. The accuracy of the temperature estimates will depend on how well the power input is known, especially the contact resistances. Further, it may be challenging to predict the influence of large metallic construction elements that may function as heat sinks.**

***Index Terms*—Heat transfer, medium voltage, ring main unit, RMU, switchgear, gas insulated switchgear, GIS, temperature rise.**

I. Introduction

ELECTRICAL equipment undergoes a rise in temperature during normal operation due to ohmic losses (neglecting iron losses). Experience has shown that when electric installations and devices, especially when housed in enclosures, shut down or malfunction, the problem often proves to be of thermal origin. The development towards more compact equipment, together with an increased focus on personnel safety (covering of live parts), leads to reduced cooling and possible subsequent overheating of the equipment.

When introducing new switchgear design, experimental temperature rise type tests have to be performed to ensure that the temperature is below the maximum limits set by the International Electrotechnical Commission (IEC 62271-1 [1]). Building prototypes and performing temperature rise tests are costly and time consuming, and development costs could be reduced if simulations could be used to predict the temperature rise and replace some of the tests.

Multiphysics tools like CFD can be used to simulate the temperature rise anywhere in the switchgear. In the literature, the reported accuracy of this method can be as good as ±2-5 K, see e.g. [2], [3]. Such tools require the detailed models of the device, and an expertise user to set up the model, mesh etc. This represents considerable resource investment in order to get a result. Another alternative, Thermal Network Method (TNM), which is based on lumped approximation of heat transfer by equivalent thermal resistors, capacitors and heat sources has lower requirements on the compute resources and corresponding calculation times, but the reported accuracy of this method is comparable to the CFD, see e.g. [4]-[6] in the hand of an expert user. The high accuracies reported for CFD and TNM are typically found when the simulations are performed with some experimental results available on similar designs as initial calibration point or as knowledge of the user. This involves adjusting the parameters to get a good fit with the experiments. Typically, this leads to an acceptable fit for the average temperatures, as there are multiple ways in which parameters can be adjusted together to achieve a consistent fit. That means the high accuracy can be expected when relatively small design changes are made to the switchgear, see e.g. [7] as the chosen parameters lead to a solution which is very close to the first solution. If the design changes are more significant, the accuracy of the model will depend on the accuracy of the estimated input parameters (e.g. contact resistances) and the experience of the person performing the simulation to adjust the heat dissipation. If temperature predictions are done on a completely new design, much lower accuracies are experienced [8].

During a development process where significant design changes are being made, setting up a CFD or TNM model might require a too high time investment compared to the reliability of the simulation results before any experimental data is available. Early in the development process, it would thus be useful to have a simplified tool to easily get a first, very quick and rough estimate of the temperature rise of the most critical parts. The scope of the work presented in this paper, was to develop such a practical design approach.

The load break switch (LBS) is a common component in the

This work was supported in part by Norwegian Research Council.

E. Fjeld and W. G. J. Rondeel are with Department of Electrical Engineering, IT and Cybernetics, University of South-Eastern Norway, Porsgrunn (e-mail: elin.fjeld@usn.no, wilhelm.rondeel@usn.no).

E. Attar and S. Singh are with ABB AS, Electrification - Distribution Solutions, Skien, Norway (e-mail: elham.attar@no.abb.com, shailendra.singh@no.abb.com).

distribution grid and one of the functional units in ring main units (RMU). The LBS typically experience the highest temperature rise as it is placed serially with the main current path and constitute a high percentage of the total resistance (many contacts and connections). The LBS can be designed in many ways, but requires minimum an open/close contact in order to function. The open/close contact will have a relatively high contact resistance, and will typically represents a thermal hot spot. The open/close contact of the LBS is thus considered a critical part, and the method focuses on estimating the temperature rise of the open/close contact of the LBS, ΔT_{LBS}, in a MV air insulated switchgear (RMU). Parts of these results have previously been presented at conferences [9]-[12].

II. Basic Theory

The steady state temperature rise is reached when the heat generating effects are balanced by the cooling effects. The heating is caused by power losses while the cooling is governed by the heat transfer mechanisms.

A. Power input

If external heat sources (as sun radiation) are not considered, the main heat source is the ohmic losses of the current path. This power loss, P, is given by:

$$P = RI_r^2 \tag{1}$$

where R is the resistance of the current path and I_r is the rated current. The resistance along the current path consist of the bulk resistance of the conductors (R_{bulk}) and the contact resistance (R_{cont}) of the connections between different conductors:

$$R = R_{bulk} + R_{cont} \tag{2}$$

In addition, losses may occur in magnetic steel near the current path (enclosure, screws, nuts, bushings etc) due to Eddy-currents and hysteresis losses. These effects may eventually be reduced or eliminated by proper design or by using nonmagnetic materials, but with some possible cost consequences.

The resistance of the conductor increases with temperature, and the resistance during load conditions, can be calculated according to

$$R_{bulk} = \rho \frac{l}{A_{cc}}(1 + \alpha \Delta T) \tag{3}$$

where ρ is the specific resistance at reference conditions, A_{cc} is the cross-sectional area of the conductor material, α is the temperature coefficient of the resistance, and ΔT is the temperature difference of the conductor between reference and load conditions. In an AC system, the effective cross-sectional area might be significantly reduced due to skin and proximity effects, see e.g. [13].

The contact resistance is due to the constriction of the current when passing from one contact member to the next, because the conductors only have metallic contact in small spots, called a-spots [14]. The contact resistance will depend on the rated current and the contact design. The combined contact resistances may contribute substantially (15 – 50 %) to the total resistance within a switchgear.

B. Power dissipation

The generated heat will be transferred to the surroundings by thermal conduction, convection and radiation. Fig. 1 illustrates the heat transfer processes for metal enclosed switchgear without ventilation openings. First, heat is transferred from the hot spots (e.g. contacts) to cooler parts (conductors, enclosed gas, enclosure walls) by conduction, radiation and convection. These three heat transfer mechanisms have different temperature dependencies, but for simplicity, sometimes a common or total heat transfer coefficient, h_{tot}, may be considered, including all three heat transfer mechanisms [10]. If we consider only the LBS, the power loss, P_{LBS}, is given by

$$P_{LBS} = h_{tot} A_{LBS} \Delta\Delta T_{LBS} \tag{4}$$

where A_{LBS} is the surface area of the LBS and $\Delta\Delta T_{LBS}$ is the over-temperature of the LBS relative to the gas inside the enclosure, defined by

$$\Delta\Delta T_{LBS} = \Delta T_{LBS} - \Delta T_{air} \tag{5}$$

where ΔT_{LBS} is the temperature rise of the LBS (relative to ambient air) and ΔT_{air} is the temperature rise of the air inside the switchgear enclosure (relative to ambient air). A lot of simplifications are made by considering a total heat transfer coefficient, as described in [10].

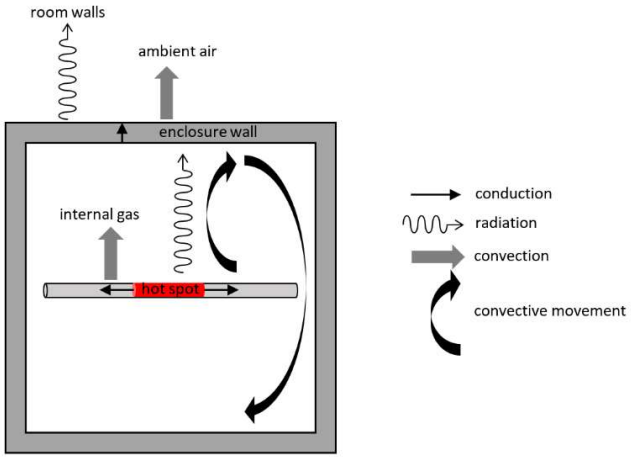

Fig. 1. Heat transfer mechanisms inside and outside a metal enclosed switchgear (without ventilation openings).

Eventually, the heat is transferred through the enclosure walls by conduction, and finally to the ambient by radiation and convection, as illustrated in Fig. 1.

III. Method Principle

For switching devices installed in a “classical” open environment (not metal enclosed), the generated heat will be transferred directly to the surroundings (ambient). The temperature rise of these switching devices could be estimated by applying empirically determined heat transfer coefficients. For switching devices installed in metal enclosed switchgear including GIS, the heat transfer process is more complicated, as illustrated in Fig. 1.

Fig. 2 shows the temperature rise of the gas surrounding the contacts (inside the enclosure) compared to the temperature rise of the open/close contact found from experiments. It can be seen that up to about 50 % of the total temperature rise of the contacts, is the temperature rise of the gas surrounding the contacts. Although it is the current path which heats the gas inside the switchgear, the basic idea of the proposed method is to use the same approach (heat transfer coefficients) for the metal enclosed case as for the open installations, but considering that the switch is now located in a "new" environment with a temperature higher compared to the ambient.

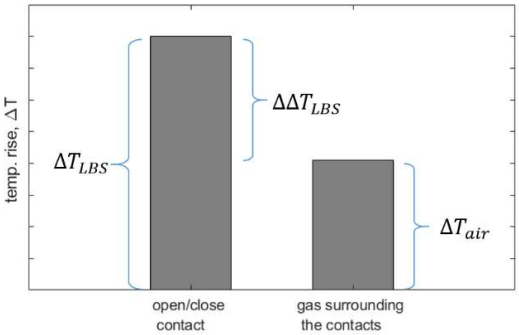

Fig. 2. Temperature rise of the open/close contact (ΔT_{LBS}) and the gas inside the gas surrounding the contacts (air inside the switchgear enclosure) (ΔT_{air}). $\Delta\Delta T_{LBS}$ represents the over-temperature of the LBS contacts relative to the gas surrounding the contacts.

The calculation is performed in three steps:

Step 1: Estimate the temperature rise of the air inside the switchgear enclosure (relative to ambient air), ΔT_{air}.
Step 2: Estimate the over-temperature of the LBS contact (relative to the air in the enclosure), $\Delta\Delta T_{LBS}$.
Step 3: Estimate the temperature rise of the open/close contact (relative to ambient air), ΔT_{LBS}, according to (5), which can be rewritten as:

$$\Delta T_{LBS} = \Delta T_{air} + \Delta\Delta T_{LBS} \quad (6)$$

The LBS does not have one uniform temperature. As the open/close contact is considered to be one of the critical parts of the LBS, the temperature rise of the open/close contact is chosen to represent the temperature rise of the LBS (ΔT_{LBS}). When this single temperature is allocated to the complete surface of the LBS, the uncertainty of the temperature is regarded to be ± 10 %.

A non-commercial prototype was custom made for the purpose of testing of the model, see Fig. 3. The dimensions of the switchgear correspond to an SF_6-filled 12/24 kV switchgear. The unit consisted of three modules. The two switch modules equipped with LBSs. The center module was equipped with a vacuum circuit breaker (VCB) in open position, and the current was thus passing from one switch module via the busbars through the second switch module. This is the normal path for the main current through the switchgear during normal conditions in a common cable ring distribution system. The switchgear operated with air at atmospheric pressure. The partially sealed enclosure was without any ventilation during the measurements. Thermal testing was carried out at the 630 A rated three-phase current, at a frequency of 50 Hz.

The background for making the estimates for each step of the model is outlined in the following sections.

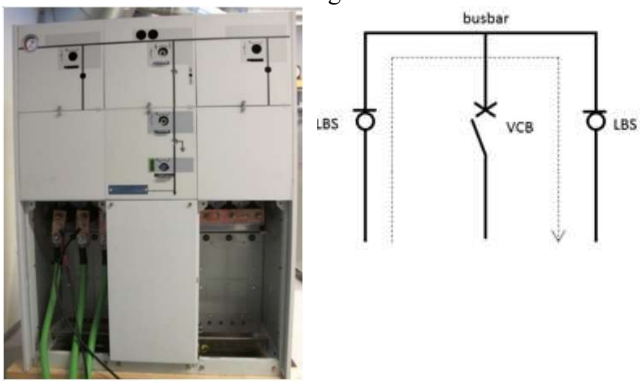

(a) (b)

Fig. 3. (a) The test object was a MV switchgear with 3 modules; two switch modules equipped with LBSs and a center module equipped with a vacuum circuit breaker (VCB) in open position. (b) Single-phase diagram of the current path through the switchgear. The current was passing from one switch module via the busbars through the second switch module, which is the path for the main current through the switchgear during normal conditions in a common cable ring distribution system.

IV. Temperature Rise of Gas Inside Enclosure (Step 1)

The temperature of the gas inside the enclosure can be estimated by applying the empirical based method provided by the IEC TR 60890 [15]. This method calculates the temperature rise of the air inside the enclosure based on the power input and the effective cooling area. The method has been developed for LV switchgear and controlgear without forced ventilation. The calculation results are accepted as verification of thermal compliance with relevant requirements in cases where measurements on the actual switchboard are unavailable. There are many similarities between LV and MV equipment, and in [12] it is shown that the method described in IEC TR 60890 could be applied as a suitable tool for making a first estimate of the temperature rise of the air inside MV equipment too.

According to the method described in IEC TR 60890, the temperature rise of the air at mid height of the enclosure ($\Delta T_{air,mid}$) is found by

$$\Delta T_{air,mid} = k \cdot d \cdot P^x \quad (7)$$

where P is the power input and k is an enclosure constant depending on the effective cooling surface of the enclosure. d is a temperature rise factor for internal horizontal partitions inside the enclosure. In case of none horizontal partitions, $d = 1$. The exponent x is 0.804 for enclosures without ventilation openings.

Further, the IEC TR 60890 suggest to estimate the air temperature rise near top of the enclosure ($\Delta T_{air,top}$) according to

$$\Delta T_{air,top} = c \cdot \Delta T_{air,mid} \quad (8)$$

where c is a temperature distribution factor. Finally, the air temperature rise at height of the LBS (ΔT_{air}) can be found by assuming a linear rise.

In order to estimate the air temperature rise according to IEC TR 60890, the dissipated power inside the enclosure, the effective cooling surface of the enclosure, and the air temperature distribution needs to be estimated. The following

sub-sections, describe how this can be done. (If the insulating gas is not air, the same approach could be applied, but new empirical data would be needed to adapt the coefficients included in IEC TR 60890.)

A. Power input

During a developing project, the total power input at steady state conditions is normally not known, and needs to be estimated. For estimating the power input, the contact resistance and bulk resistance along the current path needs to be determined. For predicting the bulk resistance, it is useful to notice that the value of the bulk resistance found by applying (3) is relatively insensitive to the exact value of the temperature increase because of the low values of the temperature coefficient, α. For example, by assuming a temperature rise of 60 K and varying this value by ± 20 %, only changes the bulk resistance of a Cu-bar by about ± 4 %. I.e. the value of the bulk resistance can be determined with quite good accuracy by applying (3) with material properties, conductor dimensions and an estimated value of the temperature rise close to the IEC limits. In addition, possible additional AC losses may have to be taken into consideration, however for secondary distribution switchgear (RMU) with currents below 1 kA, the AC losses are found to be insignificant because the conductor dimensions are about the same as the skin depth [11]. Contributions from skin and proximity effects can therefore be neglected when making a first estimate of the temperature rise of the switchgear in a secondary distribution station.

The contact resistance depends on the numbers and areas of the a-spots, which depends on the material, the surface roughness and the contact pressure. A theoretical calculation of the contact resistance is not possible, and the values have to be estimated based on experience. For the stationary connections (bolted, welded, soldered, pressed) a high force may be applied. For movable contacts (rotating, sliding, open/close), there will always be a tradeoff between friction and contact force, and these contacts typically have somewhat higher contact resistances compared to the stationary contacts. The contact resistance depends on the contact design and temperature. An accurate measurement of a single contact resistance is difficult [8], and Table 1 gives typical ranges of contact resistances found in this study.

TABLE 1
Ranges of contact resistances for MV RMU found in our study.

Type of contact :	R_{cont} [μΩ]
Bolted	1-5
Sliding/rotating	3-10
Open/close	5-10

B. Effective cooling surface

The effective surface area (A_e) is estimated by multiplying each of the enclosure surface areas (A_{surf}) by a factor b:

$$A_e = \sum A_{surf} \cdot b \qquad (9)$$

The b-factor accounts for different heat transfer for different surfaces (top, side, bottom) and whether the surfaces are exposed or covered, see Table 2.

TABLE 2
Examples of relevant surface factor b according to IEC TR 6080.

Surface :	b
Exposed top surface	1.4
Exposed side faces	0.9
Covered side faces	0.5
Floor surface	0

When the effective surface area is known, the enclosure constant (k) in (7) can be found from a diagram in IEC TR 60890. The diagram to be used in case of no ventilation openings and an effective surface area larger than 1.25 m^2, is shown in Fig. 4. For easy calculation without the need to look up in the diagram, the k-factor follows approximately a linear line given by

$$k = 0.6 - 0.125 \cdot A_e \qquad (10)$$

for effective cooling surfaces in the range 1.5 – 3.0 m^2. This range should cover RMU units with 2-5 modules (combination of switches and circuit breakers). The approximation is shown with the dotted line in Fig. 4.

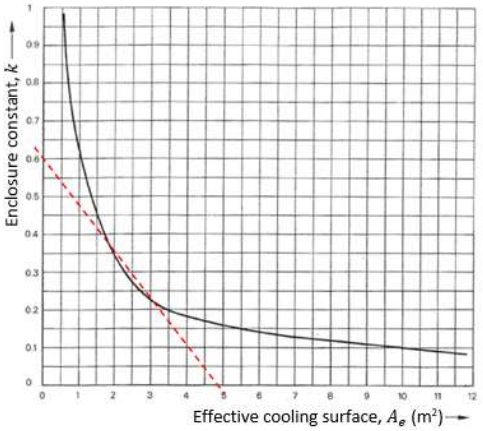

Fig. 4. Enclosure constant (k) as a function of effective cooling surface (A_e) [15]. The dotted, linear line can be used as an approximation for effective cooling surfaces in the range 1.5 – 3.0 m^2.

Previously published measurements have shown that with a known power input, the IEC-method can estimate the temperature rise of the air inside a 3-module MV switchgear 15% precision [11].

If some of the surfaces are painted (inside and/or outside), the heat transfer will increase. This might be included by multiplying the b-factor for the relevant surfaces by a factor, b_{corr}, in the range 1-1.2 depending on which of the surfaces are painted, the area of the painted surface and the increase in emissivity. Fig. 5 shows the exposed top and back surface of a 3-module switchgear painted black, and Table 3 gives examples of changes in the air temperature rise and correction factor.

Fig. 5. Switchgear enclosure surfaces painted with matt finish black paint. Back surface (left) and top surface (right).

TABLE 3
Examples of changes in temperature rise and surface correction factor for a 3-module switchgear enclosure when different surfaces are painted (increasing the emissivity from about 0.4 to nearly 1).

Painted surfaces :	$\Delta T_{air,mid}$ [K]	b_{corr} [-]
None	37	1
Top and back (outside and inside)	34	1.23

C. Air temperature distribution

When the air temperature rise at mid height is estimated according to (7), the air temperature rise near top of the enclosure ($\Delta T_{air,top}$) can (according to IEC TR 60890) be estimated according to (8) where *c* is a temperature distribution factor depending on the height/base factor (*f*)

$$f = \frac{H^{1.35}}{A_{base}} \tag{11}$$

where *H* is the enclosure height in [m] and A_{base} is the surface area of the enclosure base in [m^2]. The relationship between *c* and *f* is given in a diagram in IEC TR 60890. For easy calculation without the need to look up in diagram, it follows approximately the linear line given by

$$c = 1.2 + 0.042 \cdot f \tag{12}$$

for a separate enclosure, detached on all sides, with an effective cooling area larger than 1.25 m^2 and with *f* in the range 0.5-5.

It is important to note that the IEC method assumes a uniform distribution of the power input, which is normally close to reality for LV equipment with a number of smaller heat generating devices distributed within a switchboard. However, this is not the case for MV equipment where the heat distribution will be non-uniform due to the larger insulating distances required. The resistance across the two LBSs of a RMU in a 3 functional unit design with a circuit breaker, may accounts for about half of the total resistance per phase, and the LBSs are thus the main heat source in the switchgear. These are often located in the upper part of the switchgear to facilitate convenient operation of the switchgear. It is well known that the cooling effect of the enclosure surface depends on the relative location of the heat source [16]. If the main heat source is located in the upper or lower part of the switchgear enclosure, the *c*-factor might have to be adjusted.

In [12], CFD-simulations was performed with different heat source locations. It was found that if the heat source was located at mid height in the enclosure, the temperature distribution along the height followed a slope close to the *c*-factor found by (12). When the heat source was located in the lower part, the heat distribution was almost uniform from mid height to the top, corresponding to a *c*-factor close to 1. With the heat source in the upper part, the best fit with (8) was found with a value of *c* close to 2.

The effect of heat source location was also investigated experimentally in [12]. For the tested 3-module switchgear, the open/close contact of the LBS was located at approximately 75% height from bottom. The effect of changing the heat source location was investigated by turning the switchgear enclosure upside down, as shown in Fig. 6. The results showed a decrease of the air temperature at height of the open/close contact of 6 K [12]. This decrease is lower than expected based on the CFD-simulations with the heat source located at this height, which implies that the power input from the other parts of the current path, contributes significantly, and the difference in heat source location between the enclosure standing upright and upside down is not that significant.

Fig. 6. Front view of the test object standing upright (left) and upside down (right).

V. Over-temperature of LBS contacts (Step 2)

The over-temperature of the LBS contacts can be determined by applying empirically determined heat transfer coefficients, according to (4), which can be rewritten as

$$\Delta\Delta T_{LBS} = \frac{P_{LBS}}{h_{tot} A_{LBS}} \tag{13}$$

which correspond to the single step for equipment mounted in a "classical" open environment. The power input of the LBS, P_{LBS}, can be estimated based on the same approach as for the whole switchgear, as described in section "A. Power input.", but only considering the conductors and contacts/connections associated with the LBS. The heat emitting surface area of the LBS, A_{LBS}, must be determined from the conductor dimensions and the geometry of the switch.

The value of the heat transfer coefficient, h_{tot}, will depend on the physical dimensions of the heat source, and its orientation (vertical/horizontal). Smaller diameters typically give higher coefficients. Previously published results indicate a total heat transfer coefficient of about 17 W/m^{2}K for bare conductors with emissivity about 0.2 – 0.3 [10]. As long as we are within the relevant temperature range (i.e. close to the IEC limits), the total heat transfer coefficient doesn't seem to be very dependent on the actual temperature. However, the total heat transfer coefficient depends strongly on the emissivity of the conductors, which implies that radiation is important and needs to be taken into account. For conductors with emissivity close to 1, a total heat transfer coefficient of about 23 W/m^{2}K might have to be used [10].

For the LBS, the current path itself might be completely or partly covered by different construction elements (insulating or metallic) which are necessary for the switch to function properly, e.g. pressure cylinder, crankcase, lever, field controllers etc. These elements may influence the heat transfer from the current path to the surroundings. On the one side, the construction elements may restrict the heat transfer by

convection and radiation from the current path, depending on the design. On the other hand, the construction elements may provide an increased surface area for heat transport to the surroundings, possible also with a higher emissivity. Whether the net heat transfer from the current path will increase or decrease, depends finally on the thermal connection the construction element has to the current path.

A possible way to account for the effect of the construction elements, is to adjust the heat transfer coefficients found when only considering bare conductors:

$$h_{tot,complete} = f_{corr} \cdot h_{tot,bare} \qquad (14)$$

where f_{corr} is a correction factor. With calculation according to (14), it is still the surface area of the bare switch that should be used in (13). The value of the correction factor have to be estimated based on experimental studies. Below are some examples found in this study.

A. Insulating material

Adding encapsulation to a conductor may increase or decrease the heat transfer from the conductor, depending on the thermal conductivity of the encapsulation, the thickness / radius of the encapsulation, and the heat transfer coefficient of the external insulating surface. Fig. 7 shows a cylindrical conductor encapsulated by an insulating layer.

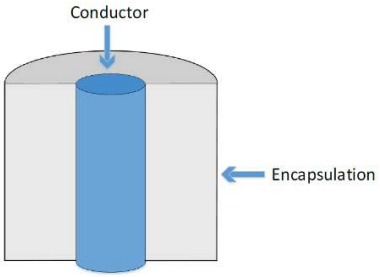

Fig. 7. Illustration of an infinitely long cylindrical encapsulated by insulating material [17].

It can be shown (see e.g. [18]) that for an infinitely long cylindrical conductor (i.e. no conduction in axial direction) covered by an insulating layer (as shown in Fig. 7), a critical radius where the heat transfer is maximum is given by:

$$r_{crit} = \frac{\lambda}{h} \qquad (15)$$

where λ is the thermal conductivity of the encapsulation and h is the heat transfer coefficient of the external surface (including both convection and radiation). An encapsulation with radius smaller than the critical radius, the encapsulation actually increases the heat transfer from the conductor surface because the heat is transferred to a larger surface for heat exchange (often also with a higher emissivity). When the radius exceeds the critical radius, the effect of the encapsulation is a decrease in the heat transfer from the conductor surface because the heat transport from the conductor to the encapsulation surface is restricted.

Two different LBS designs were tested, with different degree of encapsulation as shown in Fig. 8. The first type was a puffer switch with nearly total coverage of current path by pressure cylinder and crankcase, both made of plastic material. The gas volume between current path and plastic elements was substantial. See Fig. 8 (a). The second type was a knife blade switch with a modest part of the conductor surface covered by a mechanical grip made of plastic material with some glass filling. The gas volume between the current path and plastic material was limited. See Fig. 8 (b).

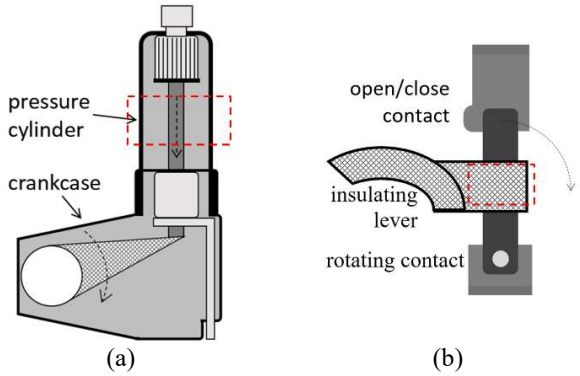

Fig. 8. Two different LBS designs where the current path is more or less covered with construction elements made of plastic material. (a) Puffer switch. (b) Knife blade switch.

Fig. 9 shows the measured temperature rise for the LBSs with and without the encapsulation. The temperature rise is changed by only a few degrees. The heat transfer coefficient was changed with less than 10 % from the bare switch (without encapsulation) and the switch with encapsulation for both LBS designs [17]. This means that the correction factor (f_{corr}) in (14) in these cases is between 0.9 – 1.1. In a rough estimate, it might not have to be considered as it is in the same order of magnitude as the uncertainty of the temperature value when a single value is used to represent the complete surface of the LBS.

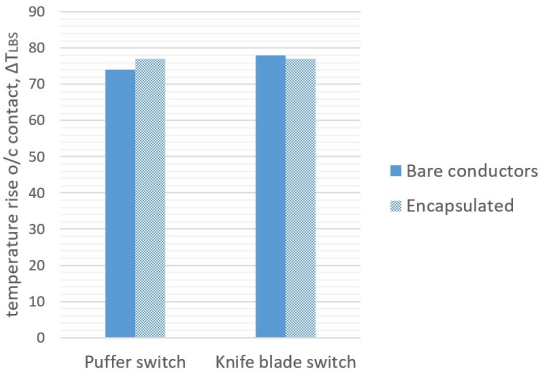

Fig. 9. Temperature rise of the open/close contact of the puffer switch and the knife blade switch for the case of bare conductors and with encapsulation partly covering the conductors; Pressure cylinder in case of puffer switch and insulating grip for the knife blade switch.

The modest influence of the encapsulation of the LBSs indicate that the encapsulation for each switch, should be around the critical radius for that switch. In order to compare the real LBS design with the simplified model in Fig. 7, only a part of the LBS is considered. The chosen areas are indicated by the boxes with dashed lines in Fig. 8 and shown in more detail in Fig. 10.

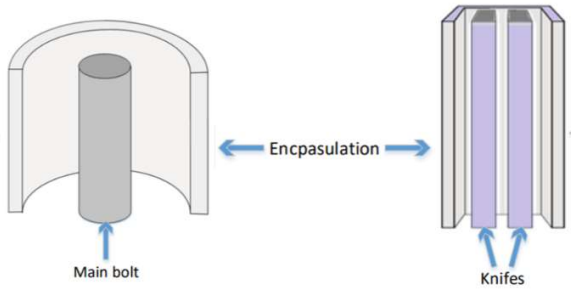

(a) (b)

Fig. 10. (a) The main bolt of the puffer switch is covered by a pressure cylinder. (b) The two parallel knifes of the knife blade switch are covered by an insulating lever [17].

For the knife blade switches, there is only a 1-2 mm air gap between the knifes and the plastic lever enclosing them. Air in such small gaps will have a lower heat transfer due to limited convection. An estimated value of the critical radius for this configuration (including the air gap and the plastic lever) is about 20 mm, which is close to the dimensions of the knife blade switch.

For the puffer switch on the other hand, there is a considerable amount of air between the main bolt and the pressure cylinder. This increased volume will increase the air flow, and the convective heat transfer is increased. This results in a larger critical radius, estimated to be in the order of 70 mm (including air gap and pressure cylinder), i.e. close to the dimensions of the puffer switch.

Based on these simplified theoretical considerations, it seems reasonable that for the LBS designs considered, the insulating encapsulation will have little influence on the heat transfer from the current path. Correction factors (f_{corr}) in the range 0.9-1.1 might therefore be assumed in (14) for these switches.

B. Metallic heat sink

An efficient heat sink will normally be made of conductive material, and can in this case not be located too close to – or bridge - the open/close gap of a switch. This may limit the cooling effect for the most critical parts. The cooling effect will depend on the location relative to the open/close contact, surface area (and cross-section), emissivity of outer surface, and the thermal connection to the current path. Two different categories of heat sinks were tested, depending on the surface area of the heat sink:

1. About the same size as the surface area of the conductive part of the LBS.
2. About twice the size of the surface area of the conductive part of the LBS.

Different construction elements can function as heat sinks. For the first category, the effect of different field controllers were tested. Without doing any modifications, these elements showed no effect on the heat transfer coefficient. This is mainly because these elements typically have a poor thermal connection to the current path and may not be placed in the direct vicinity of the open/close contact. By improving the thermal connection and the surface emissivity, a correction factor (f_{corr}) up to almost 1.2 was found. An example of field controllers tested is given in Fig. 11.

(a) (b)

Fig. 11. Example of field controllers functioning as heat sinks with surface area about the same size as the current path. (a) Original, unpainted rings with a thin steel supporting connection. (b) Modified rings painted black and with a thicker Al-connection piece.

For the second category, the plastic crankcase of the puffer switch was replaced by an Al crankcase, see Fig. 12. By simply replacing the crankcase, the effect was limited, with f_{corr} about 1.1. However, by improving the thermal connection to the current path and improving the surface emissivity, a value up to 1.3 could be found. The limited effect despite the large surface area is probably because the heat sink was located quite far from the open/close contact.

Fig. 12. Metallic crackcase functioning as heat sink with surface area about twice the size of the current path of the LBS.

Both examples illustrate the importance of ensuring an adequate thermal connection to the current path. They also show that radiation is important and a high surface emissivity of the heat sink will improve the heat transfer.

VI. Estimate Temperature Rise of LBS Contacts (Step 3)

The estimation of the temperature rise of the LBS contacts is performed by following the two steps outlined in the previous sections of this paper. The final temperature rise of the LBS contacts can then be found by adding the results from the two steps, according to (6).

The uncertainty of the estimate will depend on how well the input parameters for each step are estimated.

For step 1, the highest uncertainty is the estimate of the power input to the enclosure. The definite majority of this uncertainty comes from determining the contact resistances. If the power input is known, the IEC-model is able to predict the temperature rise of the air inside the enclosure within 15 %. Even more accurate values may be achieved if compensations are made regarding surface emissivity and non-uniform power distribution.

Uncertainty in the estimation of the power input will also affect the estimates in step no 2, but in this step, only the power input of the LBS is needed (not the complete current path). As the LBS typically contains many connections and at least one

movable contact, the uncertainty of the contact resistances will have great impact on the result.

Another main source of uncertainty in step no 2, is the determination of the total heat transfer coefficient to be applied. Experiments have shown that the value for a bare switch, i.e. only including the bare conductors of the current path, and not any other construction elements, is quite consistent. The largest uncertainty then comes from the adjustments that have to be made to account for the different construction elements, especially large metal constructions that may function as heat sinks.

Fig. 13 shows a graphical illustration of the approximate contributions from the different uncertainties to the final result of the model. An estimation can never be more precise than the uncertainty of the input parameters, which means that if there are high uncertainties related to the contact resistances or heat dissipation, simulations based on CFD or TNM will also be uncertain.

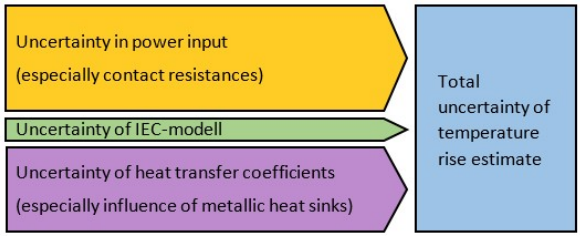

Fig. 13. Estimates of the contribution of different uncertainties to the total uncertainty of the temperature rise estimate by the proposed simplified method.

VII. Conclusion

This paper presents a practical design approach that can be used in an early stage in the development process, to get a first rough estimate of the temperature rise of the most critical parts of an air filled MV switchgear.

The method described in IEC TR 60890 is used to make a first estimate of the temperature rise of the air inside the enclosure. Then, the over-temperature of critical parts are estimated based on the application of empirically determined heat transfer coefficients. The value of the total heat transfer coefficient will depend on the surface treatment (e.g. emissivity) and the actual design. Especially the influence of large metallic structures, acting as heat sinks, might be challenging to estimate.

It should be noted that when estimating the power input, the total heat transfer coefficients and correction factors, the model assumes that we are within the relevant temperature range (i.e. close to 65/75 K temperature rise). If a device is made with a temperature rise far from the relevant temperature range, the experience based values given here will no longer be valid.

Finally, it should be mentioned that the approach presented in this paper may also be applied for SF_6 or other insulating gases, but new empirical data is then needed to adapt the coefficients included in IEC TR 60890 and to determine new values for the heat transfer coefficient.

VIII. Acknowledgment

The authors gratefully acknowledge the contributions of Master Student Stein Øygarden for his contribution in this work.

IX. References

[1] IEC Standard 62271-1: High-voltage switchgear and controlgear – Part 1: Common specifications for alternating current switchgear and controlgear, ed.2.0, 2017.

[2] S. Pawar, K. Joshi, L. Andrews and S. Kale, "Application of Computational Fluid Dynamics to Reduce the New Product Development Cycle Time of the SF_6 Gas Circuit Breaker", IEEE Trans. on Power Delivery, vol. 27, no. 1, pp.156-163, Jan. 2012.

[3] H. Song, G. Hou, W. Wang, X. Deng, Q. Huang, W. Mo, M. Hasegawa and X. Li., "Application of computational fluid dynamics to predict the temperature-rise of gas insulated switchgears," ICEPE-ST, Xi'an, 2017, pp. 694-697.

[4] X. Dong, R. Summer and U. Kaltenborn, "Thermal Network Analysis in MV GIS Design", in *Proc. CIRED Conference*, Prague, 2009, paper no 0637.

[5] S. Sing, R. Summer and U. Kaltenborn, "A Novel Approach for the Thermal Analysis of Air Insulated Switchgear", in *Proc. CIRED Conference*, Frankfurt, 2011, paper no 0492.

[6] M. Stosur, M. Szewczyk, K. Sowa, P. Dawidiowski and P. Balcerek, "Thermal behavior analyses of gas-insulated switchgear compartment using thermal network method", *IET Generation, Transmission & Distribution*, vol. 10, issue 12, p. 2833-2841, 2016

[7] M. T. Dhotre, J. Korbel, X. Ye, J. Ostrowski, S. Kotilainen and M. Kriegel, "CFD Simulation of Temperature Rise in High-Voltage Circuit Breakers", *IEEE Trans. On Power Delivery*, vol. 32, no. 6, pp. 2530-2536, Dec. 2017.

[8] M. Kriegel, E. Fjeld, A. Pedersen, P. G. Nikolic, T. Krampert, J. Snajdr, "Benchmark Case of Multiphysics Simulation for Temperature Rise Calculation", in *Proc. Int. Conf. on Condition Monitoring, Diagnosis and Maintenance* (CMDM), pp. 93-100, Bucharest, Romania, Sept. 2019.

[9] E. Fjeld, W. Rondeel and M. Saxegaard, "Temperature Rise in a Load Break Switch", in *Proc. IEEE Holm Conference*, Clearwater Beach, FL, 2016.

[10] E. Fjeld, W. Rondeel, S.T. Hagen and M. Saxegaard, "Estimating the Temperature Rise of Load Break Switch Contacts in Enclosed MV Switchgear", in *Proc. CIRED Conference*, Glasgow, 2017, paper no 0345.

[11] E. Fjeld, W. Rondeel, K. Vaagsaether, M. Saxegaard, P. Skryten, E. Attar, "Thermal Design of Future Medium Voltage Switchgear", in Proc. CIRED Conference, Lyon, 2015, paper no 1090.

[12] E. Fjeld, W. Rondeel, K. Vaagsaether and E. Attar, "Influence of heat source location on air temperatures in seald MV switchgear", in *Proc. CIRED Conference*, Glasgow, 2017, paper no 0349.

[13] X. Dong, R. Summer and U. Kaltenborn, "Thermal Network Analysis in MV GIS Design", in *Proc. CIRED Conference*, Prague, 2009, paper no 0637.

[14] R. Holm, "Electrical Contact Resistance: Fundamental Principles", in *Electric Contacts. Theory and Applications*, Berlin, Germany, Springer-Verlag, 1967, ch 1, pp. 1-4.

[15] IEC TR 60890: A method of temperature-rise verification of low-voltage switchgear and controlgear assemblies by calculation, ed.2.0, 2014.

[16] *ABB Switchgear Manual*, 10th Edition,, Cornelsen Verlag, Berlin, 2001, p. 159 .

[17] S. Oygarden, "Heat Transfer Mechanisms in MV Load Break Switches", M.S. thesis, EIK, USN, Porsgrunn, Norway, 2017.

[18] G. F. C. Rogers and Y. R. Mayhew, *Engineering Thermodynamics Work & Heat Transfer*, 4th ed. Harlow, England: Pearson Ed. Limited, 1992.